JP1.3 **Angular dependencies of GOES-derived cloud properties**

R.C. Boeke*, J.K. Ayers, R. Palikonda, R.F. Arduini
Science Systems and Applications, Inc., Hampton, VA

Patrick Minnis
Science Directorate, NASA-Langley Research Center, Hampton, VA

P.W. Heck
CIMSS, UW-Madison, Madison, WI

1. INTRODUCTION

Cloud properties retrieved from satellite imager data are used for validating climate models and are being assimilated into numerical weather prediction models. Thus, it is becoming more important to fully quantify the uncertainties in the retrieved properties. A potentially large source of error is the effect of viewing and illumination geometry on the retrievals.

Clouds observed simultaneously from different sun-target geometries can have differences in retrieved cloud properties for a variety of reasons. The vertical structure of cloud microphysics can cause viewing angle dependencies in cloud particle size retrievals because the partially absorbing channels are only sensitive to radiation from a finite path length downward from the cloud top. Microphysical heterogeneity within the cloud or 3D structure of the cloud tops can also affect the retrieval. These effects become more pronounced at high viewing or solar zenith angles. Sub-pixel cloud variability leads to biases in cloud amount when observed from large viewing angles. Because retrievals are performed using fixed ice crystal reflectance models and actual ice crystal habits can vary widely among clouds, errors can be large at particular scattering angles. The orbital positions, similarity in instrument suites, and nearly-simultaneous observations from GOES-11 and GOES-12 geostationary satellites provide a unique opportunity to assess angular dependent errors by allowing a cloud to be observed from different viewing angles at approximately the same time. This study will quantify biases in retrieved cloud properties due to viewing geometry as a function of solar zenith angle.

Biases in cloud properties increase at large viewing angles for many reasons. At certain angles, especially near direct backscatter, the water droplet phase functions are extremely sensitive to the assumed droplet size distribution (Arduini 2005). Additionally, the satellite field of view at large viewing angles can contain cloud sides and has a smaller chance of a clear line of sight than the nadir view, thus amplifying cloud 3D effects. Cloud sides can also lead to an overestimate of cloud cover for large viewing angles (Minnis 1989).

Corresponding Author Address: Robyn C. Boeke, SSAI, 1 Enterprise Parkway, Hampton, VA, 23666; email: robyn.c.boeke@nasa.gov

2. METHODOLOGY

To evaluate these issues, instantaneous .5° regional mean properties from GOES-11 and GOES-12 over the domain in Fig.1 were evaluated for the months of January and April 2009. This region was selected to obtain the maximum spatial and temporal coincidence of the GOES-11 and GOES-12 observations, and to include a wide range of viewing angles. The 0.65-μm channels on both imagers were calibrated against the Terra MODerate-resolution Imaging Spectroradiometer as in Minnis et al. (2002).

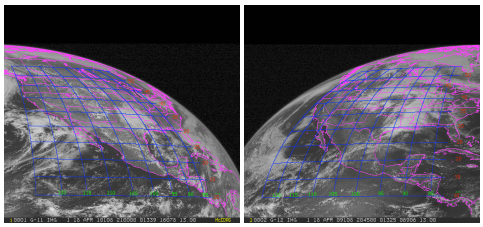

Figure 1 10°N-55°N, 82°W-125°W for GOES-11 (left) and GOES-12 (right).

Cloud properties, optical depth τ, effective height Z_{eff}, and effective droplet radius r_e or ice crystal size D_e, were retrieved using the Visible Infrared Solar-Infrared Split-window Technique (Minnis et al. 2009), which is an iterative model-matching plane-parallel technique that matches observations to theoretically calculated radiances to retrieve cloud properties. To minimize the effects of cloud heterogeneity, only single-layer overcast clouds were considered. Ice cloud properties were derived using rough ice crystal reflectance models (Yang et al., 2008) instead of the usual smooth crystal models. Additionally, the effect of partial cloudiness within grid boxes was studied to determine how it impacts the angle-dependent retrieval differences. To this end, cloud fraction was separated into fully overcast clouds (A_c=100) and four quartiles of

cloud fraction containing equal numbers of observations. To be included, the GOES-11 and GOES-12 cloud fraction agreement was required to be 0.125 or better.

3. RESULTS

Linear regression of GOES-11 vs. GOES-12 data given in Fig. 2 shows that cloud properties retrieved at large solar zenith angles are unlikely to agree. In general, cloud optical depth retrieved at large solar zenith angles for ice clouds is overestimated and biased towards either larger GOES-12 (morning) or larger GOES-11 values (evening) due to the movement of the sun over the course of the day. This is consistent with the findings of Loeb and Davies (1997), which found that there is a strong bias in optical depth that increases with solar zenith angle when clouds are assumed to be plane parallel. The effect worsens for thicker clouds. Retrievals performed at large solar zenith angles are also likely to overestimate particle size and water path and underestimate effective cloud height. These differences may be due to the use of the CO_2 channel on GOES-12 for high clouds, or due to the fact that retrievals for GOES-11 and GOES-12 are only nearly-simultaneous with a maximum 15 minute difference in scan times. The distribution for small solar zenith angles (red points) is much narrower and shows good agreement between GOES-11 and GOES-12 for the four cloud properties that were evaluated.

Hourly biases differ from daily averaged values and are lowest at local solar noon when the two satellites view the region at roughly the same scattering angles. Since the range of scattering angle pairs (shown in Fig. 3) is roughly symmetrical around solar noon, the large biases seen at terminator hours tend to cancel when averaged over the day.

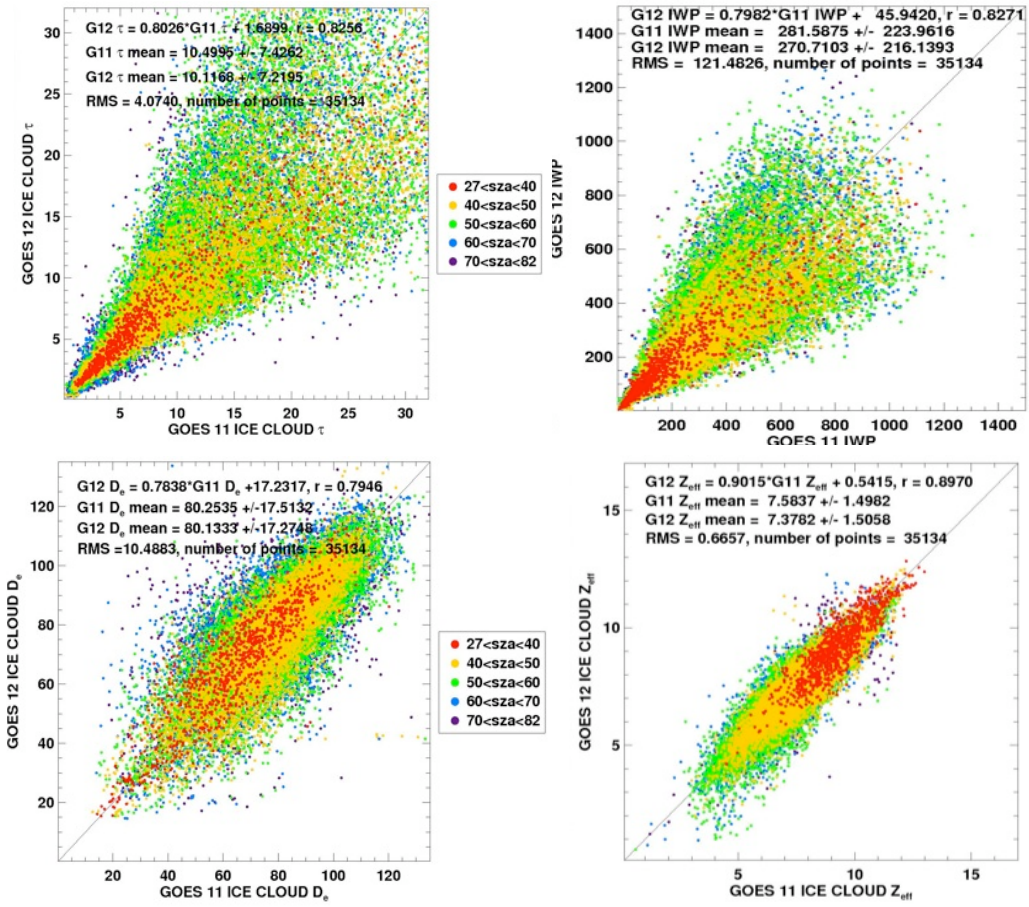

Figure 2 Linear regression of GOES-11 vs GOES-12 ice cloud properties for April 2009 color-coded by solar zenith angle.

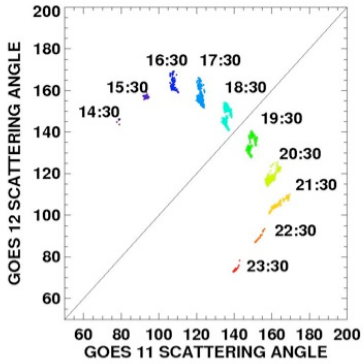

Figure 3 Hourly scattering angle pairs for GOES-11 and GOES-12

The metric used to quantify the bias between GOES-11 and GOES-12 due to viewing geometry is defined by

Bias = (*GOES-11 –GOES-12*)/GOES-11

The biases throughout the day are shown in Fig. 4. In general, ice clouds are more strongly affected by time of day and the associated scattering angle difference. At high solar zenith angles, more ice cloud sides are illuminated casting long shadows, so the retrievals are more susceptible to errors caused by 3D effects. Ice diameter biases are greatest (IBI = 0.10 – 0.15) at larger solar zenith angles, possibly due to the larger scattering angle differences that reveal radiance discrepancies between the model and actual cloud ice particle shapes.

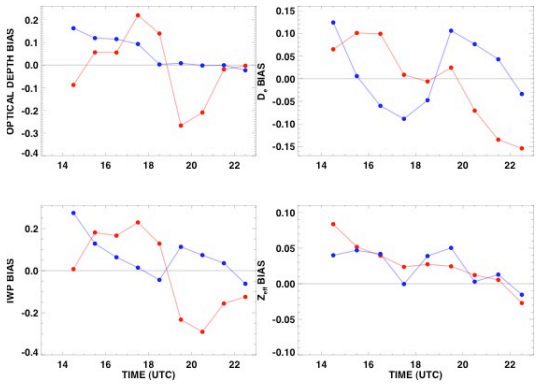

Figure 4 Hourly biases in cloud optical depth, particle size, water path, and effective cloud height for ice (red) and water (blue).

3.1 EFFECT OF PARTIAL CLOUDINESS ON BIASES CAUSED BY VIEWING GEOMETRY

Figure 5 shows biases in τ and D_e as a function of the difference between the GOES-11 and GOES-12 scattering angle. As expected, biases for partly cloudy pixels are larger than those for overcast pixels, however, at very large scattering angle differences, biases for partly cloudy pixels increase much more than those for overcast pixels. Additionally, the occurrence of outliers increases with the difference in scattering angle for partly cloudy pixels.

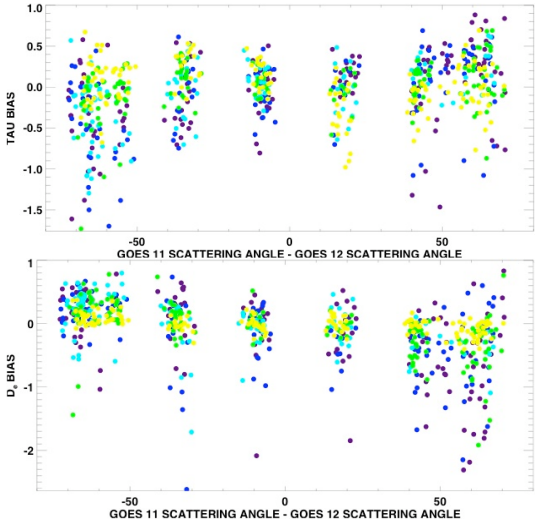

Figure 5 Biases for optical depth and ice diameter as a function of scattering angle difference. Purple: $0 < A_c \leq 13\%$, dark blue: $13 < A_c \leq 37\%$, light blue: $37 < A_c \leq 76\%$, green: $76 < A_c < 100\%$, yellow: $A_c = 100\%$.

To better quantify how the biases change with cloud fraction, box and whisker plots for scattering angle difference bins were made for each cloud cover group. Each colored plot in Figs. 6-7 corresponds with the colors for the cloud amount ranges listed in Fig. 5.

Optical depth biases for overcast clouds (both $A_c = 100\%$ and $A_c > 76\%$) are relatively small and contain few outliers, though errors increase slightly for large scattering angle differences. When moving to regions with cloud fractions less than 75.6%, biases for small scattering angle differences remain small while those having large scattering angle differences increase up to an order of magnitude.

Table 1 quantifies the optical depth biases for the largest scattering angle differences ($d\Theta < -50°$) by reporting the mean bias (*B*), a 95% confidence for the mean, and the 2-sided p-value. P-values for all but the $A_c = 100\%$ bin indicate negative biases to a confidence level of 95%. The 95% confidence interval for $A_c = 100\%$ includes zero, indicating that there is no significant bias for completely overcast clouds.

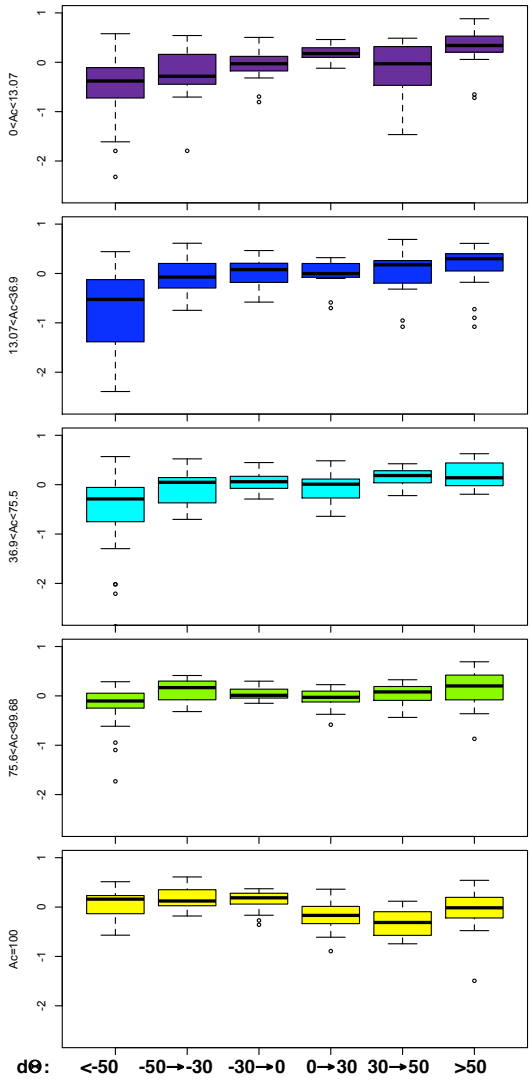

Figure 6 Optical depth biases for ranges of scattering angle difference, by percent cloud cover.

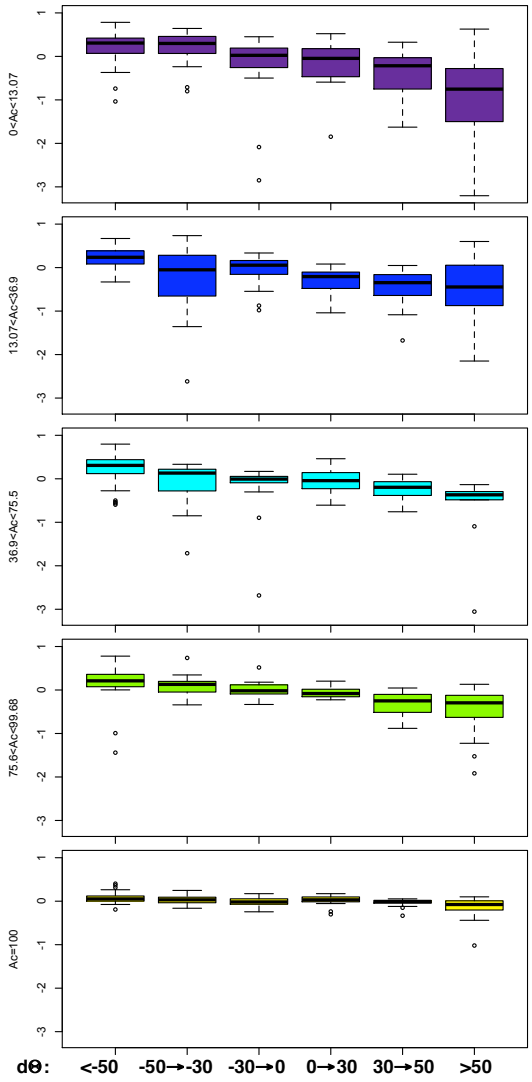

Figure 7 Ice diameter biases for ranges of scattering angle difference, by percent cloud cover.

A_c range (%)	0-13	13-37	37-76	76-99	100
B	-0.6	-1.1	-0.52	-0.17	.08
95% CI	[-0.93, -0.25]	[-1.6, -0.56]	[-0.71, -0.35]	[-0.28, -0.05]	[-0.01, 0.17]
P	0.001	1.6e-4	1.9e-6	-0.005	0.080

Table 1 Biases in τ for dΘ<-50°

A_c range (%)	0-13.	13-37	37-76	76-99	100
B	-0.93	-0.44	-0.64	-0.45	-0.14
95% CI	[-1.3, -0.6]	[-0.70, -.17]	[-1.2, -0.08]	[-.61, -0.29]	[-0.2, -0.05]
P	2e-6	0.003	0.03	2.1e-6	0.002

Table 2 Biases in D_e for dΘ>50°

Ice diameter biases are very small for A_c = 100%, but increase with scattering angle differences for any cloud fraction less than unity. For the lowest cloud fractions, the biases increase by almost an order of magnitude.

Table 2 quantifies ice diameter biases for the largest scattering angle differences (dΘ>50°). The mean biases are all negative, and 95% confidence intervals for all cloud fractions do not include zero, indicating that ice diameter bias between GOES-11 and GOES-12 will be less than zero at least 95% of the time.

4 CONCLUSIONS AND FUTURE WORK

Biases in cloud properties retrieved from satellite data due to viewing geometry are most prevalent during morning and evening, and

lowest when the sun is at its highest point for a given area. Biases during these extreme hours of the day are much smaller when the viewed scene is homogeneous and completely overcast. However, since cloud cover is often overestimated when observed from high viewing angles, a scene-by-scene analysis may be helpful to eliminate areas with partial cloud cover.

When observing areas with partial cloud cover, the optical depth and ice diameter biases increase by almost an order of magnitude for scenes where GOES-11 and GOES-12 view a pixel at significantly different scattering angles. Biases for scenes with a small difference in scattering angles are very small, and remain reasonable even for partial cloud cover. This indicates good agreement in the calibrations of the two satellites and the consistency of the retrievals despite the differences in available spectral channels.

Future work will include extending the retrievals to cover a larger domain, which will provide more angular combinations to better assess the biases . A full-seasonal comparison will be made by including additional months to cover the annual range of viewing and illumination angles. Additionally, since viewing angle biases increase with cloud inhomogeneity, multilayered clouds will be included in the study. Future retrievals will also be made using simultaneous scans from GOES-11 and GOES-12 to eliminate the effect that a 15 minute difference in scan time may cause, and parallax corrections will be applied. Lastly, cloud property retrievals that coincide with MODIS overpasses will be compared to cloud properties retrieved at a different set of angles not seen with GOES with the goal of developing a correction for cloud properties retrieved at various viewing angles.

This type of analysis only yields the differences between one set of angles and another. To assess the overall angle-dependent error relative to the actual uncertainty in each measurement, the results will need to be compared to a ground truth measurement. This process will also be pursued in future analyses.

Acknowledgments
This research was supported by the NASA Modeling and Analysis Program and the Department of Energy ARM Program through DE-AI02-07ER64546.

5 REFERENCES

Arduini, R.F., P. Minnis, W.L. Smith, Jr., J.K. Ayers, M.M. Khaiyer, and P.W. Heck: Sensitivity of satellite-retrieved cloud properties to the effective variance of cloud droplet size distribution, *Proc. 15th Annual ARM Sci. Team Mtg,* Daytona Beach, FL, March 14-18, 2005.

Ayers, J.K., R. Palikonda, M.M. Khaiyer, P.Minnis, L. Nyugen, and W.L. Smith, Jr., 2006: Angular dependence of cloud property retrievals from satellite data, *Proc. AMS 14th Conf. Satellite Meteorol. And Oceanog.,* Atlanta, GA, 29 Jan. – 2 Feb. 2006.

Loeb, N. G. and R. Davies, 1997: Angular dependence of observed reflectances: a comparison with plane parallel theory, *J. Geophys. Res.*, **102**, 6865-6881.

Minnis, P., 1989: Viewing zenith angle dependence of cloudiness determined from coincident GOES East and GOES West Data", *Journal of Geophysics Research*, Vol 94, NO D2, pp 2303-2320.

Minnis, P., et al., 2001: A near-real time method for deriving cloud and radiation properties from satellite for weather and climate studies, *Proc. AMS 11th Conf. on Satellite Meteorology and Oceanography*, Madison, WI, October 15-18.

Minnis, P., et al., 2002: Rapid calibration of operational and research meteorological satellite imagers, Part I: Evaluation of research satellite visible channels as references. *J. Atmos. Oceanic Technol.*, **19**, 1233-1249.

Minnis, P., et al., 2009: CERES Edition-2 cloud property retrievals using TRMM VIRS and Terra and Aqua MODIS data, Part I: Algorithms. Submitted to *IEEE Trans. Geosci. Remote Sens.*

Yang, P., G. W. Kattawar, G. Hong, P. Minnis, and Y. X. Hu, 2008: Uncertainties associated with the surface texture of ice particles in satellite-based retrieval of cirrus clouds: Part I. Single-scattering properties of ice crystals with surface roughness. *IEEE Trans. Geosci. Remote Sens.*, **46**, 1940-1947, doi:10.1109/ TGRS.2008.916471.